Anti-hypersensitive effect of angiotensin (1-7) on streptozotocin-induced diabetic neuropathic pain in mice

（マウスにおけるストレプトゾトシン誘発性糖尿病性神経障害性疼痛におけるアンジオテンシン (1-7) の抗痛覚過敏効果）

申請者　弘前大学大学院医学研究科
脳神経科学領域　神経生理学教育研究分野

氏名　　小潟　佳輝
指導教授　上野　伸哉

Abstract

Background: We have recently reported that the spinal angiotensin (Ang) converting enzyme (ACE)/Ang II/AT1 receptor axis and downstream p38 MAPK phosphorylation are activated in streptozotocin (STZ)-induced diabetic mice and leads to tactile hypersensitivity. Moreover, our previous results suggested that the intrathecal (i.t.) administration of Ang (1-7), an N-terminal fragment of Ang II, may attenuate the Ang II-induced nociceptive behaviour through the inhibition of p38 MAPK phosphorylation via Mas receptors. Here, we investigated whether the i.t. administration of Ang (1-7) can attenuate STZ-induced diabetic neuropathic pain.

Methods: Tactile and thermal hypersensitivities were determined using the von Frey filament and Hargreaves tests, respectively. The protein expression of ACE2, Mas receptors and phospho-p38 MAPK was measured by Western blotting. Spinal ACE2 activity was determined using ACE2 activity assay kit.

Results: The i.t. administration of Ang (1-7) significantly reduced the tactile and thermal hypersensitivities on day 14 after STZ injection and these effects were significantly prevented by the Mas receptor antagonist A779. The expression of ACE2 and Mas receptors in the plasma membrane fraction of the lumbar dorsal spinal cord were both significantly decreased in STZ mice. Spinal ACE2 activity was also decreased while p38 MAPK phosphorylation was increased in the lumbar dorsal region of these mice. This

phosphorylation was attenuated by the injection of Ang (1-7), whose effect was reversed by A779.

Conclusions: Our data demonstrate that Ang (1-7) attenuates STZ-induced diabetic neuropathic pain and that this occurs though a mechanism involving spinal Mas receptors and the inhibition of p38 MAPK phosphorylation.

1. Introduction

Diabetic neuropathy is one of the major complications of diabetes mellitus and affects half of all diabetes patients (Barrett et al., 2007; Veves et al., 2008). According to published papers, 50 to 60% of patients with diabetic neuropathy experience neuropathic pain (Abbott et al., 2011; Galer et al., 2000; Gordois et al., 2003). Although there are many pharmacological approaches to treat diabetic neuropathic pain, most of them are not effective for controlling painful symptoms (Javed et al., 2015; Ray et al., 2004; Zimmermann et al., 2003). Therefore, novel therapeutic targets are required for the treatment of diabetic neuropathic pain.

The renin angiotensin (Ang) system (RAS) is well known as the key regulator of fluid balance and electrolyte homeostasis (Kobori et al., 2007). In the RAS, renin cleaves angiotensinogen to Ang I which is further converted to Ang II by Ang converting enzyme (ACE) (Atlas, 2007; George et al., 2010; Sparks et al., 2014). Ang II is a main bioactive component of the RAS and exerts its actions by binding to two G protein-coupled receptors, the Ang II type 1 (AT1) and Ang II type 2 (AT2) receptors. There is increasing evidence that shows the involvement of the Ang II system in the modulation of nociceptive information. In the dorsal root ganglia (DRG) of rats with chronic constriction injury, the activation of AT2 receptors result in an increase in the phosphorylation of p38 mitogen-activated protein kinase (p38 MAPK) and extracellular signal-regulated kinase (ERK),

which are involved in the maintenance of hypersensitivity (Smith et al., 2013). On the other hand, although AT2 receptors are not involved in pain transmission in the spinal cord, a nociceptive behaviour was shown to be induced by the intrathecal (i.t.) administration of Ang II and p38 MAPK phosphorylation to be mediated by AT1 receptors (Nemoto et al., 2013). Also, we have revealed that the spinal ACE/Ang II/AT1 receptor pathway and subsequent p38 MAPK phosphorylation were involved in the streptozotocin (STZ)-induced diabetic mouse model, and led to tactile hypersensitivity (Ogata et al., 2016). These findings indicate that Ang II promotes spinal pain transmission via AT1 receptors.

Ang (1-7), an N-terminal fragment of Ang II, is directly produced from Ang II by the action of ACE2 and binds to G protein-coupled Mas receptors. By acting on Mas receptors, Ang (1-7) exerts counter-regulatory effects on the ACE/Ang II/AT1 receptor pathway including vasodilation, anti-proliferation and anti-inflammation (Santos et al., 2013; Simões e Silva et al., 2013). In our previous study, the i.t. administration of Ang (1-7) antagonized the Ang II-induced nociceptive behaviour and was accompanied by an inhibition of p38 MAPK phosphorylation that was mediated through Mas receptors (Nemoto et al., 2014). However, the potential effect of Ang (1-7) on STZ-induced neuropathic pain remains unknown.

Therefore, the aim of this study is to determine whether an i.t. injection of Ang (1-7) can attenuate the tactile and thermal hypersensitivities observed in the STZ-induced

diabetic mouse model. In addition, we demonstrate that the spinal ACE2/Ang (1-7)/Mas receptor axis is altered in STZ mice.

2. Materials and methods

2.1. Animals

Male ddY mice (Japan SLC, Japan), weighing between 26 and 30 g were used throughout this study. Mice were housed in cages with free access to food and water under conditions of constant temperature (22 ± 2 ºC) and humidity (55 ± 5%), with a 12 h light-dark cycle (lights on: 8:00 to 20:00). Groups of 11-12 mice for behavioural experiments, 7-8 mice for reverse transcriptase-polymerase chain reaction (RT-PCR), and 7-9 mice for Western blotting were used in single experiments. All experiments were performed following the approval from the Ethics Committee of Animal Experiment in Hirosaki University, and Tohoku Medical and Pharmaceutical University and according to the National Institutes of Health Guide for the Care and Use of Laboratory Animals. Efforts were made to minimize suffering and to reduce the number of animals used.

2.2. Induction of diabetes

STZ (Sigma-Aldrich, USA) was dissolved in 0.1 N citrate buffered saline (pH 4.5) and injected into mice at the dose of 200 mg/kg through the intravenous (i.v.) route (Ogata et

al., 2016). Age-matched control mice were injected with vehicle alone.

2.3. Intrathecal injections

The i.t. injections were carried out as previously described (Nemoto et al., 2013, 2014, 2015a, 2015b; Ogata et al., 2016). The i.t. injections were made in unanaesthetized mice at the L5, L6 intervertebral space as described by Hyden and Wilcox (1980). Briefly, a volume of 5 μl was administered i.t. with a 28-gauge needle connected to a 50-μl Hamilton microsyringe, the animal being lightly restrained to maintain the position of the needle. Puncture of the dura was indicated behaviourally by a slight flick of the tail.

2.4. von Frey filament test

Tactile hypersensitivity was determined by assessing paw withdrawal in the von Frey filament test as previously described (Ogata et al., 2016). Mice were placed on a mesh floor inside a clear plastic cubicle for an acclimatization period of a least 30 min before the test. After adaptation, the von Frey filament (applied pressure by each filament: 0.07, 0.16, 0.4, 0.6, 1.0 and 1.4 g) was pressed perpendicularly against the plantar surface of the left and right hind paw from beneath the mesh floor and held for 3 seconds with the filament slightly buckled. A positive response was noted if the paw was sharply withdrawn. Whenever a positive response to a stimulus occurred, the next smaller von Frey hair was

applied, and whenever a negative response occurred, the next higher force was applied. Ambulation was considered an ambiguous response, and in such cases the stimulus was repeated. The scores were averaged trials to determine mean left and right paw values for each mice.

The effect of A779 on Ang (1-7)-induced anti-tactile hypersensitivity was assessed using a stimulation of equal intensity (0.4 g filament) that was applied 10 times to the plantar surface of the left and right hind paw at intervals of 5-10 seconds. The frequency of sharp withdrawal responses was measured.

2.5. Hargreaves test

Thermal hypersensitivity was assessed using Hargreaves test (Hargreaves et al., 1988). Radiant heat to the planter surface of a hind paw was applied from underneath the glass floor using a high intensity light bulb and the latency time to elicit paw withdrawal was measured with an electronic timer (Ugo Basile, Italy). The stimulation intensity was adjusted to yield a baseline paw withdrawal latency of 10 ± 1 sec for Ringer-treated vehicle mice. The cutoff was set at 20 sec to avoid tissue damage. The average of three measurements taken at 1-min intervals was calculated.

2.6. Drugs and antibodies

The following drugs and reagents were used: Ang (1-7) (Peptide Institute, Japan); [D-Ala^7]-Ang (1-7) (A779) (Bachem, Switzerland); sodium pentobarbital (Kyoritsu Seiyaku Co., Japan); rabbit monoclonal antibodies against ERK 1/2, phospho-ERK1/2, c-Jun N-terminus kinase (JNK), phospho-JNK, p38 MAPK, phospho-p38 MAPK, and horseradish peroxidase (HRP)-conjugated goat anti-rabbit IgG antibody (Cell Signaling Technology, USA); rabbit anti-ACE2 polyclonal antibody (21115-1-AP; Proteintech, USA); rabbit anti-Mas receptor polyclonal antibody (AAR-013; Alomone Laboratories, Israel); rabbit anti-alpha1 Na^+/K^+-ATPase monoclonal antibody (ab76020; Abcam, UK); Go Taq qPCR Master mix (Promega, USA); enhanced chemiluminescence (ECL) assay kit (GE Healthcare, UK). For i.t. injections, Ang (1-7) and A779 was dissolved in Ringer's solution (Fuso Pharmaceutical Industries, Japan). The specificity of the anti-Mas receptor and anti-ACE2 antibodies used in this study have been demonstrated using Mas receptor knockout mice (Freund et al., 2012) and ACE2-siRNA transfected cells (Li et al., 2017), respectively. The antibody against the membrane-bound anti-Na^+/K^+-ATPase used in our study has been reported to selectivity bind the protein in membrane fractions but not with cytoplasmic fractions (Aravena et al., 2012; Planès et al., 2016).

2.7. RT-PCR

Total RNA was isolated from the spinal cord and kidney of mice using the TRI Reagent

(Sigma-Aldrich) according to the manufacturer's protocol. Total RNA was reverse-transcribed using ReverTraAce (Toyobo, Japan) and oligo (dT) primers (Thermo Fisher Scientific, USA). Primers with the following sequences were used for PCR: ACE2 forward primer 5'-ACT ACA GGC CCT TCA GCA AA-3' and reverse primer 5'-TGC CCA GAG CCT AGA GTT GT-3' (205 bp product); Mas receptor forward primer 5'-CTC TCC ACC TCC TGA CTG TT-3' and reverse primer 5'- GCC TCC TTG AGA AGT AGC TG-3' (175 bp product); and glyceraldehyde-3-phosphate dehydrogenase (GAPDH) forward primer 5'-ACC ACA GTC CAT GCC ATC AC-3' and reverse primer 5'-TCC ACC ACC CTG TTG CTG TA-3' (166 bp product). For a qualitative assessment of PCR products, an aliquot from each reaction was resolved by electrophoresis through an agarose gel followed by staining with ethidium bromide. An image of each gel was digitally captured using a FLA-3000 image analyzer (Fujifilm, Japan). For the quantification of mRNA expression, real-time PCR was carried out in a 20 μl solution containing Go Taq qPCR Master mix (10 μl), cDNA synthesized above (2 μl), water (7 μl) and primers (1 μl) using the StepOnePlus Real-Time PCR System (Applied Biosystems, USA). The amount of product in each ACE2 and Mas receptor PCR was normalized to the amount of GAPDH product.

2.8. Preparation of whole cell lysate and membrane fraction

Mice were decapitated under anesthesia and then the whole spinal cord was expelled

by pressure using a syringe and physiological saline. A subcellular fractionation procedure was performed according to previous reports (Garção et al., 2014; Goebel-Goody et al., 2009; Phillips et al., 2001). Briefly, the tissue samples were homogenized in a glass grinding vessel using a Teflon-glass homogenizer (Dounce Tissue Grinder, Wheaton, USA) at 4°C in homogenization buffer (pH 6.0, 0.32 M sucrose, 20 mM Tris, 0.1 mM CaCl2, 1 mM MgCl2) with Complete™ Protease Inhibitor Cocktail EDTA-free (Roche Diagnostics, Germany). A portion of each homogenate was collected as whole cell lysate while the remaining portion was centrifuged at 1,000×g for 10 min at 4°C to remove nuclei and unbroken cells. The supernatant was transferred to a new tube and centrifuged at 10,000×g for 15 min at 4°C to obtain the membrane-enriched pellet. The whole cell lysate and membrane-enriched pellet were resuspended in homogenization buffer and solubilized by the addition of sodium dodecyl sulfate (SDS) to a final concentration of 1%. To avoid contamination of each fractions, supernatants were centrifuged 3 times and the pellets were washed with homogenization buffer. Protein concentration was determined by the Bradford protein assay (Bio-Rad Laboratories, USA).

2.9. Western blotting

Dorsal lumbar spinal cord and DRG (L4-L6) samples were taken 14 days after STZ injection. Western blotting was performed as previously described (Nemoto et al., 2013,

2014, 2015a, 2017; Ogata et al., 2016). Equal amounts of protein were denatured in SDS sample buffer. Electrophoresis was performed in 7.5% acrylamide gels for the detection of ACE2; 10% acrylamide gels were used in all other cases. Proteins were transferred electrically from the gel onto a polyvinylidene difluoride membrane using a semi-dry blotting apparatus (Bio-Rad Laboratories, USA). The blots were blocked for 30 min with 5% skim-milk in Tris-buffered saline supplemented with 0.01% Tween-20 (TBST), and incubated with rabbit antibodies against ERK1/2, phospho-ERK1/2, JNK, phospho-JNK, p38 MAPK, phospho-p38 MAPK, Mas receptors, ACE2 (diluted 1:1000 with TBST containing 5% skim-milk), or alpha1 Na^+/K^+-ATPase (diluted 1:5000 with TBST containing 5% skim-milk) overnight at 4°C. Afterwards, the blots were washed several times and then incubated at room temperature for 2 h with HRP-conjugated anti-rabbit IgG antibody (diluted 1:5000 with TBST containing 5% skim-milk). Blots were developed using an ECL assay kit, and immunoreactive proteins visualized on Hyper-film ECL. The density of the corresponding bands was analyzed using Image-J 1.43u (National institute of Health).

2.10. Measurement of ACE2 activity

Lumbar dorsal spinal cord samples were taken 14 days after STZ injection. Measurement of ACE2 activity (SensoLyte 390 ACE2 activity assay kit, AnaSpec, USA)

was performed according to the supplied manual. Briefly, spinal cord tissues were homogenized in Component C buffer of the kit. Homogenized samples were incubated for 15 min at 4°C, followed by centrifugation at 20,000×g for 10 min. The supernatants were collected and stored at -80°C until measurement of ACE2 activity. Total protein concentration was quantified using the Bradford protein assay.

2.11. Statistical methods

Data are expressed as means ± SEM. Significant differences were analyzed by a one-way or two-way analysis of variance (ANOVA), followed by Fisher's PLSD test for multiple-comparisons. Student's t-test was used for comparisons between two groups. In all comparisons, $p < 0.05$ was considered statistically significant.

3. Results

3.1. Effect of Ang (1-7) on STZ-induced tactile hypersensitivity

The von Frey filament test was used first to examine whether the i.t. administration of Ang (1-7) can inhibit the tactile hypersensitivity induced in mice by STZ. Tactile hypersensitivity was assessed before (pre) and 15, 30, 60, 90, 120 and 150 min after the injection of Ang (1-7) at the doses of 3 or 30 pmol in both STZ- and vehicle-treated mice. In the latter, Ang (1-7) did not affect the paw withdrawal threshold during the 150-min

post-observation period (Figure 1A). In contrast, Ang (1-7) significantly inhibited the tactile hypersensitivity observed in STZ mice and showed a maximum effect 90 min after the injection with either doses (Figure 1B). Ang (1-7) (30 pmol) completely attenuates STZ-induced tactile hypersensitivity (Figure S1). Next, we investigated whether Mas receptors might play a role in the anti-hypersensitive effect of Ang (1-7) by co-administering (i.t.) the receptor antagonist A779 90 min before the behavioural measurements. As shown in Fig. 1C, the anti-hypersensitive effect of Ang (1-7) (30 pmol) was significantly prevented by A779 (0.1 and 1 nmol), whereas A779 alone did not affect either vehicle- or STZ-treated mice. In addition, these treatments did not affect the withdrawal responses in naive mice at all (Figure 1C). These results suggest that Ang (1-7) attenuates STZ-induced tactile hypersensitivity and this effect is mediated through spinal Mas receptors.

3.2. Effect of Ang (1-7) on STZ-induced thermal hypersensitivity

We examined the effect of Ang (1-7) on thermal hypersensitivity observed in STZ mice using Hargreaves test. Thermal hypersensitivity was assessed before (pre) and 30, 60, 90, 120, 150, 180 and 240 min after the injection of Ang (1-7) (30 pmol) or Ang (1-7) (30 pmol) in combination with A779 (1 nmol) in both STZ- and vehicle-treated mice. In the latter, neither Ang (1-7) nor Ang (1-7) in combination with A779 affected the paw

withdrawal latency during the 240-min post-observation period (Figure 2A). In contrast, the injection of Ang (1-7) significantly inhibited the thermal hypersensitivity observed in STZ mice and showed a maximum effect after 90 min while this effect was abolished by A779 (Figure 2B). Ninety min after the i.t. injection, the decrease in withdrawal latency in STZ mice, but not in naive and vehicle-treated mice, was significantly attenuated by Ang (1-7), which was reversed by A779 (Figure 2C). These results suggest that Ang (1-7) attenuates the STZ-induced thermal hypersensitivity and that this effect is mediated through spinal Mas receptors.

3.3. Effect of Ang (1-7) or Ang (1-7) in combination with the Mas receptor antagonist A779 on the phosphorylation of MAPKs in the lumbar dorsal spinal cord of STZ mice

Recently, we have revealed that, in mice with STZ-induced diabetes, the increase in spinal Ang II leads to an increase in phosphorylated p38 MAPK and neuropathic pain (Ogata et al., 2016). Moreover, the phosphorylation of other MAPKs such as ERK1/2 and JNK are also known to be involved in the STZ-induced hyperalgesia (Middlemas et al., 2006; Tsuda et al., 2008). Thus, Western blotting was used here to investigate the effect of Ang (1-7) or Ang (1-7) in combination with A779 on the phosphorylation of spinal ERK1/2, JNK and p38 MAPK in STZ mice. On day 14 after STZ injection, the phosphorylation of all three MAPK was found to be significantly increased in the lumbar dorsal cord when

compared to vehicle-injected control mice (Figure 3A), while it was not significantly changed in the DRG (Figure S2A-C). The i.t. administration of Ang (1-7) (30 pmol) significantly attenuated the phosphorylation of only p38 MAPK, which was prevented by the i.t. administration of A779 (1 nmol) (Figure 2D). In contrast, neither Ang (1-7) nor Ang (1-7) in combination with A779 affected the phosphorylation of ERK1/2 and JNK (Figure 3B and C). These results suggest that Ang (1-7) attenuates the phosphorylation of p38 MAPK in the lumbar dorsal spinal cord of STZ mice via Mas receptors without altering the phosphorylation of ERK1/2 and JNK.

3.4. Alterations in Mas receptor and ACE2 expression in the lumbar dorsal spinal cord of STZ mice

To support the likelihood that ACE2 and Mas receptors are expressed in the lumbar spinal cord, we confirmed the presence of their mRNA transcript in untreated mice by RT-PCR (Figure 4A). The kidney was used as a positive control for mRNA detection. Next, using real-time quantitative RT-PCR, we determined whether changes in Mas receptor and ACE2 mRNAs occurred in the lumbar dorsal spinal cord of STZ mice and found that both transcripts were significantly decreased compared with vehicle mice (Figure 4B and C).

ACE2 is a transmembrane protein and it cleaves Ang II to generate the N-terminal peptide Ang (1-7) that can bind Mas receptors that are expressed on the plasma membrane

(Guy et al., 2005). We used Western blotting to examine the possible accompanying changes in Mas receptor and ACE2 protein levels in the spinal plasma membrane fraction of STZ mice. Indeed, we observed that in this fractions both ACE2 and Mas receptor protein levels were significantly decreased in STZ mice compared with vehicle mice (Figure 4D and E). In contrast to the spinal cord, the expression of Mas receptors was not changed in the DRG (FigureS3).

3.5. Alteration in ACE2 activity in the lumbar dorsal spinal cord of STZ mice

We also examined whether the ACE2 activity was altered in the lumbar dorsal spinal cord of STZ mice using the SensoLyte 390 ACE2 activity assay kit. As shown in Table 1, spinal ACE2 activity was significantly decreased in STZ mice compared with vehicle-treated control mice.

4. Discussion and conclusions

It has recently been shown that peripheral but not i.t. administration of Ang II causes hypersensitivity (Shepherd et al., 2018a). While it was suggested that the induction of neuropathic pain involves the activation of AT2 receptors in DRGs (Smith et al., 2016), other reports indicate that it involves AT2 receptors on peripheral macrophages (Shepherd et al., 2018b). As, the action site of Ang II is still debated and requires further studies, we

have investigated pain transmission from the perspective of the spinal Ang system. We have recently reported that the expression of spinal ACE is increased in STZ mice, which in turn leads to an increase in Ang II levels. Though AT1 receptor signaling, the elevated spinal Ang II levels produced tactile hypersensitivity and was accompanied by the phosphorylation of p38 MAPK (Ogata et al., 2016). We have also reported that the nociceptive behaviour induced in mice by an i.t. administration of Ang II was attenuated by the i.t. administration of Ang (1-7) which acted through Mas receptors and the inhibition of p38 MAPK phosphorylation (Nemoto et al., 2014). Nonetheless, the effect of Ang (1-7) and the involvement of the ACE2/Ang (1-7)/Mas receptor axis on tactile hypersensitivity observed in STZ mice remained unclear. Therefore, we used this diabetic mouse model to show for the first time that Ang (1-7) has beneficial effects on diabetic neuropathic pain.

STZ is widely used to induce experimental diabetes in rodents which will display neuropathic pain similar to the symptoms observed in diabetic patients (Calcutt and Chaplan, 1997; Mert et al., 2015; Tesfaye et al., 1996). The neuropathic pain induced by STZ has been reported to be alleviated by insulin treatment (Messinger et al., 2009), while there are indications that STZ affects the vanilloid receptor family of ion channels in DRG neurons independently of its ability to induce hyperglycemia (Pabbidi et al., 2008). In our previous experiment, a single i.v. injection of a low dose of STZ (2 or 20 mg/kg) caused transient tactile hypersensitivity 1-3 days later without affecting blood glucose levels

(Ogata et al., 2016). On the other hand, 200 mg/kg of STZ caused long-lasting tactile hypersensitivity concurrent with an increase in blood glucose levels (Ogata et al., 2016). To exclude the possibility raised above that STZ is acting directly on neurons (Pabbidi et al., 2008), we studied mice on day 14 after the STZ (200 mg/kg) injection, a point in time that showed a marked decrease in pain threshold.

The RAS consists of two counter-regulatory axes, the ACE/Ang II/AT1 receptor axis and the ACE2/Ang (1-7)/Mas receptor axis. The activation of the ACE/Ang II/AT1 receptor axis causes deleterious effects such as vasoconstriction, inflammation, fibrosis, cellular growth and migration of vascular smooth muscle cells, while the ACE2/Ang (1-7)/Mas receptor axis opposes these effects (Ferreira et al., 2010; Kim and Iwao, 2000; Mehta and Griendling, 2007; Santiago et al., 2010; Simões e Silva et al., 2013). In the mouse model of STZ-induced diabetes, the upregulation of the ACE/Ang II/AT1 receptor axis and downregulation of the ACE2/Ang (1-7)/Mas receptor axis have been observed in the retina, and this imbalance is associated with the progression of retinopathy (Verma et al., 2012). Moreover, the quantity of ACE is increased, while that of ACE2 is decreased in kidneys of diabetic patients and mice (Mizuiri et al., 2010; Shi et al., 2015). These reports suggest that the imbalance between the ACE/Ang II/AT1 receptor axis and the ACE2/Ang (1-7)/Mas receptor axis may be responsible for the development and/or progression of diabetic complications.

In this study, we showed that ACE2 and Mas receptor transcripts were significantly decreased in the lumbar dorsal spinal cord of STZ mice compared with vehicle mice. Accordingly, the protein expression of ACE2 and Mas receptor proteins were also significantly decreased in the spinal plasma membrane fraction of STZ mice. Moreover, spinal ACE2 activity was decreased by almost 20% in STZ mice. These results suggest that the ACE2/Ang (1-7)/Mas receptor axis is down-regulated in the spinal cord of STZ mice. As we have previously demonstrated that the ACE/Ang II/AT1 receptor axis is up-regulated in the spinal cord of these mice (Ogata et al., 2016), it appears that an imbalance between these two axes is involved in the STZ-induced diabetic neuropathic pain.

Chronic nerve injury-induced neuropathic pain was shown to be attenuated by the i.t. administration of Ang (1-7) and signaling via spinal Mas receptors (Zhao et al., 2015). In the present study, we showed for the first time that the i.t. administration of Ang (1-7) significantly reduced STZ-induced tactile and thermal hypersensitivities, and that these effects were significantly prevented by A779. Moreover, we have recently demonstrated that Mas receptors are present on neurons and microglia but are absent from astrocytes in the superficial dorsal horn (Nemoto et al., 2017). Together, our results suggest that Ang (1-7) attenuates the STZ-induced diabetic neuropathic pain and that this action is mediated by Mas receptors on spinal neurons and microglia. Forte et al. (2016) have revealed that Mas receptors are expressed in the DRG and the femur extrudate of a cancer-induced bone

pain mouse model, and that Ang (1-7) attenuates the pain via Mas receptors in both regions. In our study, the expression of Mas receptors was not changed in the DRG of STZ mice compared with vehicle-treated mice. Therefore, there is a possibility that Ang (1-7) produced its anti-hypersensitive effect in STZ mice through Mas receptors in both the lumbar dorsal spinal cord and DRGs.

It has been demonstrated that MAPKs, including p38 MAPK, JNK and ERK1/2, become phosphorylated in the spinal cord of STZ-induced experimental diabetic models, thereby leading to neuropathic pain (Daulhac et al., 2006; Middlemas et al., 2006; Tsuda et al., 2008). However, Ang II induced the phosphorylation of p38 MAPK but not JNK and ERK1/2 in the spinal cord (Nemoto et al., 2015a; Ogata et al., 2016). In the present study, we have shown in agreement with previous studies that all three phospho-p38 MAPK, -JNK and -ERK1/2 were significantly increased in the dorsal lumbar spinal cord of STZ mice. Among these, only phospho-p38 MAPK was markedly decreased by Ang (1-7), an effect significantly prevented by A779. These results suggest that Ang (1-7) attenuates the phosphorylation of p38 MAPK observed in the lumbar dorsal spinal cord of STZ mice which is mediated through spinal Mas receptors. Since the i.t. injection of Ang (1-7) did not affect the phosphorylation of neither ERK nor JNK, it may possible that Ang (1-7) attenuates only the phosphorylation of p38 MAPK induced by Ang II through AT1 receptors.

The present study showed that in STZ mice injected with Ang (1-7), A779 only partially prevented the attenuation of the rise in spinal p38 MAPK phosphorylation whereas it almost completely blocked the anti-hypersensitive effect. Interestingly, it has been reported that Ang (1-7) increases intracellular nitric oxidase (NO) levels in catecholaminergic neurons, and this effect can also be attenuated by a pretreatment with A779 (Yang et al., 2011). The hyperalgesia induced by prostaglandin E2 in rats was also inhibited following an intraplantar injection of Ang (1-7) which activated the L-arginine/NO/cyclic GMP pathway and subsequent ATP-sensitive K^+ channels (Costa et al., 2014). Thus, it may be postulated that in STZ mice, the anti-hypersensitive effect induced by Ang (1-7) involves spinal Mas receptor and the combination of downstream pathways, inhibitory (e.g. p38 MAPK phosphorylation) and activating (e.g. L-arginine/NO/cyclic GMP and ATP-sensitive K^+ channels).

In conclusion, we show that the ACE2/Ang (1-7)/Mas receptor axis is down-regulated in the spinal cord of STZ mice and that an imbalance between this axis and the ACE/Ang II/AT1 receptor axis is critical for the STZ-induced neuropathic pain. Moreover, since the i.t. administration of Ang (1-7) significantly attenuated the STZ-induced diabetic neuropathic pain, the activation of the ACE2/Ang (1-7)/Mas receptor axis could be an effective therapeutic target to alleviate the neuropathic pain in diabetic patients.

Acknowledgements

We are grateful to Professor Mitsuo Tanabe, Dr. Shun Watanabe and Ms. Misa Oyama (Laboratory of Pharmacology, School of Pharmaceutical Sciences, Kitasato University, Tokyo, Japan) for their teaching in the isolation of DRGs from mice.

Author contributions

K.T. designed the research. Y.O., W.N., O.N., R.Y. and S.S. conducted experiments. Y.O., W.N. and K.T wrote the manuscript. K.T., T.F. and S.U. supervised the experiments.

References

Abbott, C.A., Malik, R.A., van Ross, E.R., Kulkarni, J., Boulton, A.J. (2011). Prevalence and characteristics of painful diabetic neuropathy in a large community-based diabetic population in the U.K. Diabetes Care 34, 2220-2224.

Aravena, C., Beltrán, A.R., Cornejo, M., Torres, V., Díaz, E.S. et al. (2012). Potential role of sodium-proton exchangers in the low concentration arsenic trioxide-increased intracellular pH and cell proliferation. PLoS One 7, e51451.

Atlas, S.A. (2007). The renin-angiotensin aldosterone system: pathophysiological role and pharmacologic inhibition. J Manag Care Pharm 13, 9-20.

Barrett, A.M., Lucero, M.A., Le, T., Robinson, R.L., Dworkin, R.H., Chappell, A.S. (2007). Epidemiology, public health burden, and treatment of diabetic peripheral neuropathic pain: a review. Pain Med 8, S50-S62.

Calcutt, N.A., Chaplan, S.R. (1997). Spinal pharmacology of tactile allodynia in diabetic rats. Br J Pharmacol 122, 1478-1482.

Costa, A., Galdino, G., Romero, T., Silva, G., Cortes, S., Santos, R., Duarte, I. (2014). Ang-(1-7) activates the NO/cGMP and ATP-sensitive K^+channels pathway to induce peripheral antinociception in rats. Nitric Oxide 37, 11-16.

Daulhac, L., Mallet, C., Courteix, C., Etienne, M., Duroux, E., Privat, A.M., Eschalier, A., Fialip, J. (2006). Diabetes-induced mechanical hyperalgesia involves spinal mitogen-

activated protein kinase activation in neurons and microglia via N-methyl-D-aspartate-dependent mechanisms. Mol Pharmacol 70, 1246-1254.

Ferreira, A.J., Castro, C.H., Guatimosim, S., Almeida, P.W., Gomes, E.R. et al. (2010). Attenuation of isoproterenol-induced cardiac fibrosis in transgenic rats harboring an angiotensin-(1-7)-producing fusion protein in the heart. Ther Adv Cardiovasc Dis 4, 83-96.

Forte, B.L., Slosky, L.M., Zhang, H., Arnold, M.R., Staatz, W.D., Hay, M., Largent-Milnes, T.M., Vanderah, T.W. (2016). Angiotensin-(1-7)/Mas receptor as an antinociceptive agent in cancer-induced bone pain. Pain 157, 2709-2721.

Freund, M., Walther, T., von Bohlen und Halbach, O. (2012). Immunohistochemical localization of the angiotensin-(1-7) receptor Mas in the murine forebrain. Cell Tissue Res 348, 29-35.

Galer, B.S., Gianas, A., Jensen, M.P. (2000). Painful diabetic polyneuropathy: epidemiology, pain description, and quality of life. Diabetes Res Clin Pract 47, 123-128.

Garção, P., Oliveira, C.R., Cunha, R.A., Agostinho, P. (2014). Subsynaptic localization of nicotinic acetylcholine receptor subunits: a comparative study in the mouse and rat striatum. Neurosci Lett 566, 106-110.

George, A.J., Thomas, W.G., Hannan, R.D. (2010). The renin-angiotensin system and

cancer: old dog, new tricks. Nat Rev Cancer 10, 745-759.

Goebel-Goody, S.M., Davies, K.D., Alvestad Linger, R.M., Freund, R.K., Browning, M.D. (2009). Phospho-regulation of synaptic and extrasynaptic N-methyl-d-aspartate receptors in adult hippocampal slices. Neuroscience 158, 1446-1459.

Gordois, A., Scuffham, P., Shearer, A., Oglesby, A., Tobian, J.A. (2003). The health care costs of diabetic peripheral neuropathy in the U.S. Diabetes Care 26, 1790-1795.

Guy, J.L., Lambert, D.W., Warner, F.J., Hooper, N.M., Turner, A.J. (2005). Membrane-associated zinc peptidase families: comparing ACE and ACE2. Biochim Biophys Acta 1751, 2-8.

Hargreaves, K., Dubner, R., Brown, F., Flores, C., Joris, J. (1988). A new and sensitive method for measuring thermal nociception in cutaneous hyperalgesia. Pain 32, 77-88.

Hylden, J.L., Wilcox, G.L. (1980). Intrathecal morphine in mice: a new technique. Eur J Pharmacol 67, 313-316.

Javed, S., Petropoulos, I.N., Alam, U., Malik, R.A. (2015). Treatment of painful diabetic neuropathy. Ther Adv Chronic Dis 6, 15-28.

Kim, S., Iwao, H. (2000). Molecular and cellular mechanisms of angiotensin II-mediated cardiovascular and renal diseases. Pharmacol Rev 52, 11-34.

Kobori, H., Nangaku, M., Navar, L.G., Nishiyama, A. (2007). The intrarenal renin-angiotensin system: from physiology to the pathobiology of hypertension and kidney

disease. Pharmacol Rev 59, 251-287.

Mehta, P.K., Griendling, K.K. (2007). Angiotensin II cell signaling: physiological and pathological effects in the cardiovascular system. Am J Physiol Cell Physiol 292, C82-C97.

Mert, T., Oksuz, H., Tugtag, B., Kilinc, M., Sahin, E., Altun, I. (2015). Anti-hypernociceptive and anti-oxidative effects of locally treated dobutamine in diabetic rats. Pharmacol Rep 67, 1016-1023.

Messinger, R.B., Naik, A.K., Jagodic, M.M., Nelson, M.T., Lee, W.Y. et al. (2009). In vivo silencing of the CaV3.2 T-type calcium channels in sensory neurons alleviates hyperalgesia in rats with streptozocin-induced diabetic neuropathy. Pain 145, 184-195.

Middlemas, A.B., Agthong, S., Tomlinson, D.R. (2006). Phosphorylation of c-Jun N-terminal kinase (JNK) in sensory neurones of diabetic rats, with possible effects on nerve conduction and neuropathic pain: prevention with an aldose reductase inhibitor. Diabetologia 49, 580-587.

Mizuiri, S., Hemmi, H., Arita, M., Aoki, T., Ohashi, Y. et al. (2010). Increased ACE and decreased ACE2 expression in kidneys from patients with IgA nephropathy. Nephron Clin Pract 117, C57-C66.

Nemoto, W., Nakagawasai, O., Yaoita, F., Kanno, S., Yomogida, S., Ishikawa, M., Tadano, T., Tan-No, K. (2013). Angiotensin II produces nociceptive behavior through spinal

AT1 receptor-mediated p38 mitogen-activated protein kinase activation in mice. Mol Pain 9, 38.

Nemoto, W., Ogata, Y., Nakagawasai, O., Yaoita, F., Tadano, T., Tan-No, K. (2014). Angiotensin (1-7) prevents angiotensin II-induced nociceptive behaviour via inhibition of p38 MAPK phosphorylation mediated through spinal Mas receptors in mice. Eur J Pain 18, 1471-1479.

Nemoto, W., Ogata, Y., Nakagawasai, O., Yaoita, F., Tadano, T., Tan-No, K. (2015a). Involvement of p38 MAPK activation mediated through AT1 receptors on spinal astrocytes and neurons in angiotensin II- and III-induced nociceptive behavior in mice. Neuropharmacology 99, 221-231.

Nemoto, W., Ogata, Y., Nakagawasai, O., Yaoita, F., Tanado, T., Tan-No, K. (2015b). The intrathecal administration of losartan, an AT1 receptor antagonist, produces an antinociceptive effect through the inhibiton of p38 MAPK phosphorylation in the mouse formalin test. Neurosci Lett 585, 17-22.

Nemoto, W., Yamagata, R., Ogata, Y., Nakagawasai, O., Tadano, T., Tan-No, K. (2017). Inhibitory effect of angiotensin (1-7) on angiotensin III-induced nociceptive behaviour in mice. Neuropeptides 65, 71-76.

Ogata, Y., Nemoto, W., Nakagawasai, O., Yamagata, R., Tadano, T., Tan-No, K. (2016). Involvement of spinal angiotensin II system in streptozotocin-induced diabetic

neuropathic pain in mice. Mol Pharmacol 90, 205-213.

Pabbidi, R.M., Cao, D.S., Parihar, A., Pauza, M.E., Premkumar, L.S. (2008). Direct role of streptozotocin in inducing thermal hyperalgesia by enhanced expression of transient receptor potential vanilloid 1 in sensory neurons. Mol Pharmacol 73, 995-1004.

Phillips, G.R., Huang, J.K., Wang, Y., Tanaka, H., Shapiro, L. et al. (2001). The presynaptic particle web: ultrastructure, composition, dissolution, and reconstitution. Neuron 32, 63-77.

Planès, R., Ben Haij, N., Leghmari, K., Serrero, M., BenMohamed, L., Bahraoui, E. (2016). HIV-1 Tat protein activates both the MyD88 and TRIF pathways to induce tumor necrosis factor alpha and interleukin-10 in human monocytes. J Virol 90, 5886-5898.

Ray, W.A., Meredith, S., Thapa, P.B., Hall, K., Murray, K.T. (2004). Cyclic antidepressants and the risk of sudden cardiac death. Clin Pharmacol Ther 75, 234-241.

Santiago, N.M., Guimarães, P.S., Sirvente, R.A., Oliveira, L.A., Irigoyen, M.C., Santos, R.A., Campagnole-Santos, M.J. (2010). Lifetime overproduction of circulating angiotensin-(1-7) attenuates deoxycorticosterone acetate-salt hypertension-induced cardiac dysfunction and remodeling. Hypertension 55, 889-896.

Santos, R.A., Ferreira, A.J., Verano-Braga, T., Bader, M. (2013). Angiotensin-converting enzyme 2, angiotensin-(1-7) and Mas: new players of the renin-angiotensin system. J Endocrinol 216, R1-R17.

Shepherd, A.J., Copits, B.A., Mickle, A.D., Karlsson, P., Kadunganattil, S. et al. (2018a). Angiotensin II triggers peripheral macrophage-to-sensory neuron redox crosstalk to elicit pain. J Neurosci 38, 7032-7057.

Shepherd, A.J., Mickle, A.D., Golden, J.P., Mack, M.R., Halabi, C.M. et al. (2018b). Macrophage angiotensin II type 2 receptor triggers neuropathic pain. Proc Natl Acad Sci U S A 115, E8057-E8066.

Shi, Y., Lo, C.S., Padda, R., Abdo, S., Chenier, I. et al. (2015). Angiotensin-(1–7) prevents systemic hypertension, attenuates oxidative stress and tubulointerstitial fibrosis, and normalizes renal angiotensin-converting enzyme 2 and Mas receptor expression in diabetic mice. Clin Sci 128, 649-663.

Simões e Silva, A.C., Silveira, K.D., Ferreira, A.J., Teixeira, M.M. (2013). ACE2, angiotensin-(1-7) and Mas receptor axis in inflammation and fibrosis. Br J Pharmacol 169, 477-492.

Smith, M.T., Wyse, B.D., Edwards, S.R. (2013). Small molecule angiotensin II type 2 receptor (AT2R) antagonists as novel analgesics for neuropathic pain: comparative pharmacokinetics, radioligand binding, and efficacy in rats. Pain Med 14, 692-705.

Smith, M.T., Anand, P., Rice, A.S. (2016). Selective small molecule angiotensin II type 2 receptor antagonists for neuropathic pain: preclinical and clinical studies. Pain 157, S33-S41.

Sparks, M.A., Crowley, S.D., Gurley, S.B., Mirotsou, M., Coffman, T.M. (2014). Classical renin-angiotensin system in kidney physiology. Compr Physiol 4, 1201-1228.

Tesfaye, S., Malik, R., Harris, N., Jakubowski, J.J., Mody, C., Rennie, I.G., Ward, J.D. (1996). Arterio-venous shunting and proliferating new vessels in acute painful neuropathy of rapid glycaemic control (insulin neuritis). Diabetologia 39, 329-335.

Tsuda, M., Ueno, H., Kataoka, A., Tozaki-Saitoh, H., Inoue, K. (2008). Activation of dorsal horn microglia contributes to diabetes-induced tactile allodynia via extracellular signal-regulated protein kinase signaling. Glia 56, 378-386.

Verma, A., Shan, Z., Lei, B., Yuan, L., Liu, X. et al. (2012). ACE2 and Ang-(1-7) confer protection against development of diabetic retinopathy. Mol Ther 20, 28-36.

Veves, A., Backonja, M., Malik, R.A. (2008). Painful diabetic neuropathy: epidemiology, natural history, early diagnosis, and treatment options. Pain Med 9, 660-674.

Li, W, Wang, R., Ma, J.Y., Wang, M., Cui, J. et al. (2017). A human long non-coding RNA ALT1 controls the cell cycle of vascular endothelial cells via ACE2 and cyclin D1 pathway. Cell Physiol Biochem 43, 1152-1167.

Yang, R.F., Yin, J.X., Li, Y.L., Zimmerman, M.C., Schultz, H.D. (2011). Angiotensin-(1-7) increases neuronal potassium current via a nitric oxide-dependent mechanism. Am J Physiol Cell Physiol 300, C58-C64.

Zhao, Y., Qin, Y., Liu, T., Hao, D. (2015). Chronic nerve injury-induced Mas receptor

expression in dorsal root ganglion neurons alleviates neuropathic pain. Exp Ther Med 10, 2384-2388.

Zimmermann, U., Kraus, T., Himmerich, H., Schuld, A., Pollmächer, T. (2003). Epidemiology, implications and mechanisms underlying drug-induced weight gain in psychiatric patients. J Psychiatr Res 37, 193-220.

Figure legends

Figure 1. Effect of Ang (1-7) on STZ-induced tactile hypersensitivity in mice. Tactile hypersensitivity was assessed on day 14 after STZ (200 mg/kg) injection. Time course of the effect of i.t. administration of Ang (1-7) on the paw withdrawal response to von Frey filaments in (A) vehicle- or (B) STZ-injected mice. (A) Two-way ANOVA: Ang (1-7) treatment ($F_{2,33} = 0.13$, $p > 0.05$), time ($F_{6,198} = 0.56$, $p > 0.05$), Ang (1-7) treatment × time ($F_{12,198} = 0.42$, $p > 0.05$). (B) Two-way ANOVA: Ang (1-7) treatment ($F_{2,32} = 15.98$, $p < 0.01$), time ($F_{6,192} = 19.73$, $p < 0.01$), Ang (1-7) treatment × time ($F_{12,192} = 5.87$, $p < 0.01$). One-way ANOVA: pre, $F_{2,32} = 0.39$, $p > 0.05$; 15 min, $F_{2,32} = 5.82$, $p < 0.01$; 30 min, $F_{2,32} = 4.58$, $p < 0.05$; 60 min, $F_{2,32} = 19.57$, $p < 0.01$; 90 min, $F_{2,32} = 19.51$, $p < 0.01$; 120 min, $F_{2,32} = 7.28$, $p < 0.01$; 150 min, $F_{2,32} = 1.38$, $p > 0.05$. Values represent the means ± S.E.M. for 11-12 mice. $^{**}p < 0.01$ compared with Ringer controls. (C) Effect of the i.t. injection of Ang (1-7), A779 or Ang (1-7) in combination with A779 on the frequency of the paw withdrawal response to a 0.4 g tactile stimuli in naive, vehicle- and STZ-injected mice. Ringer's solution, Ang (1-7), A779 or Ang (1-7) in combination with A779 was administered 90 min prior to measurements. Two-way ANOVA: treatment ($F_{5,162} = 9.54$, $p < 0.01$), group ($F_{2,162} = 613.72$, $p < 0.01$), treatment × group ($F_{10,162} = 12.87$, $p < 0.01$). One-way ANOVA: $F_{17,162} = 84.37$, $p < 0.01$. Values represent the means ± S.E.M. for 6-12 mice. $^{**}p < 0.01$ compared with Ringer-injected vehicle mice, $^{\#\#}p < 0.01$ compared with

Ringer-injected STZ mice and $$$p < 0.01$ compared with Ang (1-7) (30 pmol)-injected STZ mice.

Figure 2. Effect of Ang (1-7) on STZ-induced thermal hypersensitivity in mice. Thermal hypersensitivity was assessed on day 14 after STZ (200 mg/kg) injection. Time course of the effect of an i.t. administration of Ang (1-7) or Ang (1-7) in combination with A779 on the paw withdrawal latency to radiant heat in (A) vehicle- or (B) STZ-injected mice. (A) Two-way ANOVA: treatment ($F_{2,15} = 2.16$, $p > 0.05$), time ($F_{7,105} = 0.99$, $p > 0.05$), treatment × time ($F_{14,105} = 0.94$, $p > 0.05$). (B) Two-way ANOVA: treatment ($F_{2,15} = 9.00$, $p < 0.01$), time ($F_{7,105} = 5.96$, $p < 0.01$), treatment × time ($F_{14,105} = 2.90$, $p < 0.01$). One-way ANOVA: pre, $F_{2,15} = 0.54$, $p > 0.05$; 30 min, $F_{2,15} = 0.20$, $p < 0.01$; 60 min, $F_{2,15} = 5.91$, $p < 0.05$; 90 min, $F_{2,15} = 12.85$, $p < 0.01$; 120 min, $F_{2,15} = 5.71$, $p < 0.05$; 150 min, $F_{2,15} = 1.27$, $p > 0.05$; 180 min, $F_{2,15} = 5.54$, $p < 0.05$; 240 min, $F_{2,15} = 2.44$, $p > 0.05$. Values represent the means ± S.E.M. for 6 mice. $**p < 0.01$ compared with Ringer controls and $##p < 0.01$, $#p < 0.05$ compared with Ang (1-7) (30 pmol). (C) Effect of the i.t. injection of Ang (1-7), A779 or Ang (1-7) in combination with A779 on the frequency of the paw withdrawal response to radiant heat in naive, vehicle- and STZ-injected mice. Ringer's solution, Ang (1-7), A779 or Ang (1-7) in combination with A779 was administered 90 min prior to measurements. Two-way ANOVA: treatment ($F_{3,60} = 7.87$, $p < 0.01$), group ($F_{2,60}$

= 106.87, $p < 0.01$), treatment × group ($F_{6,60} = 7.04$, $p < 0.01$). One-way ANOVA: $F_{11,60} = 25.42$, $p < 0.01$. Values represent the means ± S.E.M. for 6 mice. **$p < 0.01$ compared with Ringer-injected vehicle mice, ##$p < 0.01$ compared with Ringer-injected STZ mice and \$\$$p < 0.01$ compared with Ang (1-7) (30 pmol)-injected STZ mice.

Figure 3. Phosphorylation of MAPKs in the lumbar dorsal spinal cord of STZ mice. The phosphorylation state of ERK1/2, JNK and p38 MAPK was measured 90 min following the i.t. administration of vehicle, 30 pmol Ang (1-7) alone or in combination with 1 nmol A779, A779 alone on day 14 after STZ (200 mg/kg) or vehicle injection. (A) Representative Western blots of total- and phospho-MAPKs. (B-D) Quantitative analysis of the Western blots showing the fold-changes in (B) phospho-ERK1/2, (C) -JNK and (D) -p38 MAPK relative to total-ERK1/2, JNK and p38 MAPK, respectively, and further normalized to the vehicle-injected group. Two-way ANOVA: group ($F_{1,17} = 24.91$, $p < 0.01$), Ang (1-7) treatment ($F_{1,17} = 5.82$, $p < 0.05$), group ×Ang (1-7) treatment ($F_{1,17} = 6.87$, $p < 0.05$). One-way ANOVA: $F_{3,17} = 11.14$, $p < 0.01$. Values represent the means ± S.E.M. for groups of 4-6 mice. *$p < 0.05$ and **$p < 0.01$ compared with Ringer-injected vehicle mice, ##$p < 0.01$ compared with Ringer-injected STZ mice, \$$p < 0.05$ compared with Ang (1-7)-injected STZ mice.

Figure 4. The mRNA expression and protein levels for both Mas receptor and ACE2 are decreased in the lumber dorsal spinal cord of STZ mice. (A) Total RNA was extracted from the lumbar dorsal spinal cord (lane 1 and 2) and kidney (lane 3) of naïve mice followed by the detection of Mas receptor and ACE2 mRNA by RT-PCR, gel electrophoresis and imaging. GAPDH mRNA was used as a positive control for expression. Determination of the relative levels of (B) Mas receptor mRNA and (C) ACE2 mRNA by real-time quantitative RT-PCR in the mouse lumbar dorsal spinal cord. Dorsal spinal cord samples were collected on day 14 after STZ injection then proteins extracted. (D, E) Top: Representative Western blots of plasma membrane Mas receptors (MasR) and ACE2 in the lumbar area. Bottom: Relative quantification of Mas receptors and ACE2 to Na^+/K^+-ATPase set as 1.0 in the vehicle mice. Na^+/K^+-ATPase expression was used as a membrane marker and loading control. Values represent the means ± S.E.M. for groups of 7-9 mice. $*p < 0.05$, $**p < 0.01$ compared with vehicle mice.

Table 1. ACE2 activity in lumbar dorsal spinal cord of STZ mice.

Experimental group	ACE2 activity (RFU/μg protein)	Activity relative to vehicle (%)
Vehicle (N = 9)	847.4 ± 44.9	100
STZ (N = 9)	680.8 ± 47.0*	80.3

Spinal ACE2 activity was measured on day 14 after STZ (200 mg/kg) injection. *$p < 0.05$ compared with vehicle control.

Figure 1

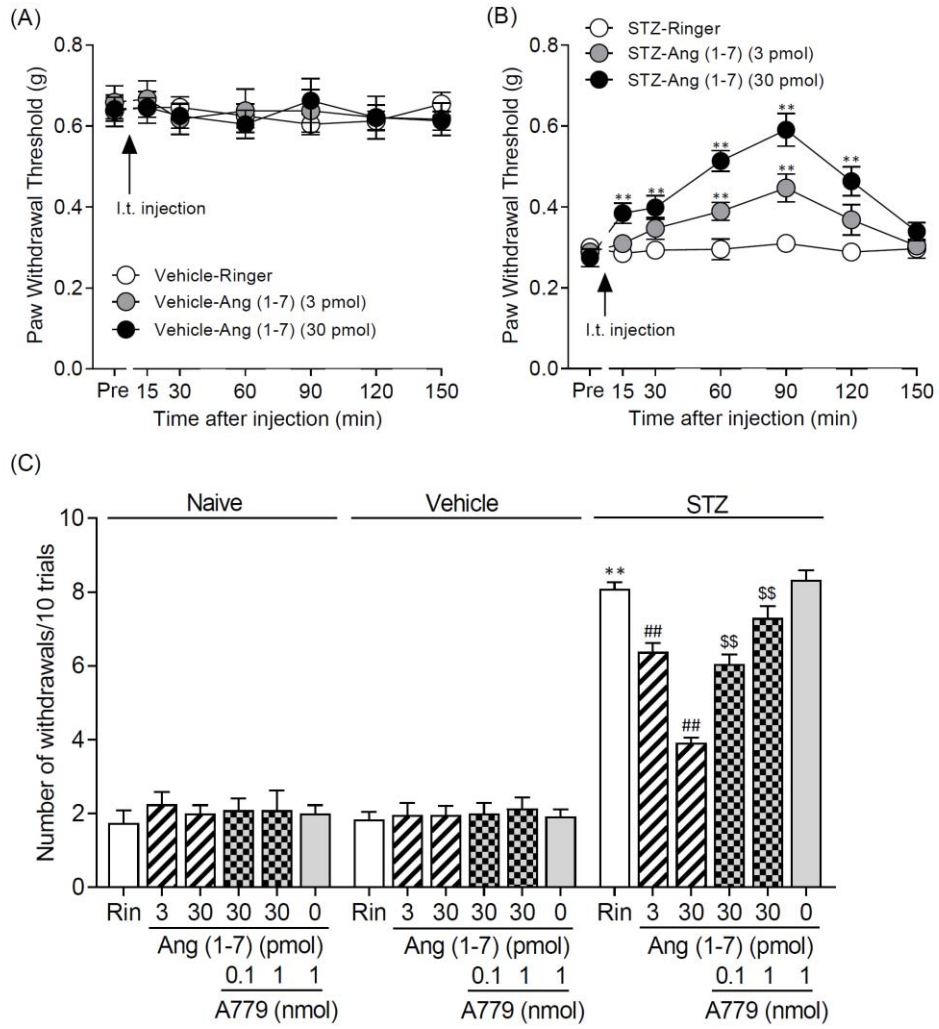
(A)
Paw Withdrawal Threshold (g)
0.8
0.6
0.4
0.2
0.0
I.t. injection
Vehicle-Ringer
Vehicle-Ang (1-7) (3 pmol)
Vehicle-Ang (1-7) (30 pmol)
Pre 15 30 60 90 120 150
Time after injection (min)
(B)
STZ-Ringer
STZ-Ang (1-7) (3 pmol)
STZ-Ang (1-7) (30 pmol)
Paw Withdrawal Threshold (g)
I.t. injection
Pre 15 30 60 90 120 150
Time after injection (min)
(C)
Naive
Vehicle
STZ
Number of withdrawals/10 trials
10
8
6
4
2
0
Rin 3 30 30 30 0
Ang (1-7) (pmol)
0.1 1 1
A779 (nmol)

Figure 2

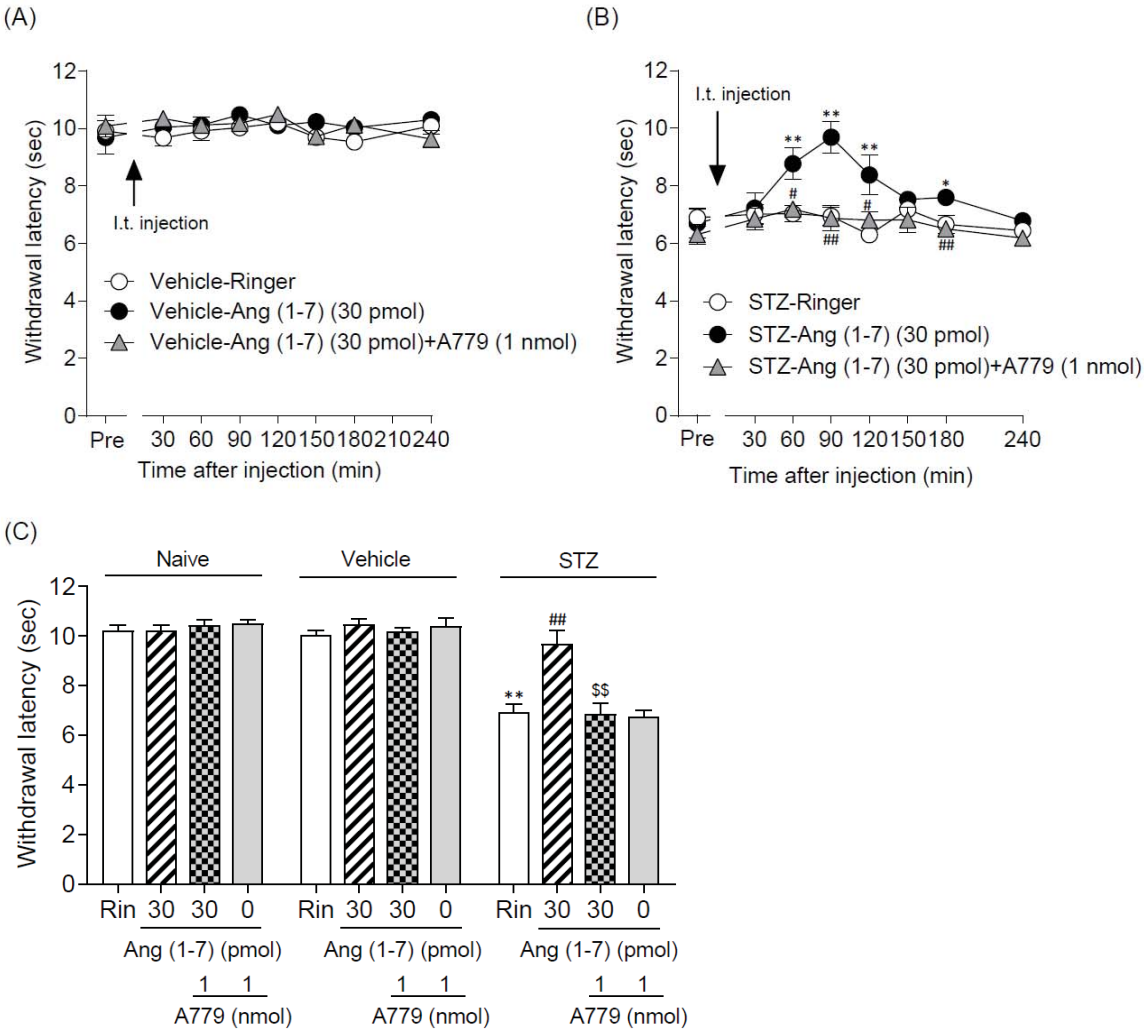
(A)
Withdrawal latency (sec)
I.t. injection
Vehicle-Ringer
Vehicle-Ang (1-7) (30 pmol)
Vehicle-Ang (1-7) (30 pmol)+A779 (1 nmol)
Pre 30 60 90 120 150 180 210 240
Time after injection (min)
(B)
I.t. injection
STZ-Ringer
STZ-Ang (1-7) (30 pmol)
STZ-Ang (1-7) (30 pmol)+A779 (1 nmol)
Pre 30 60 90 120 150 180 240
Time after injection (min)
(C)
Naive
Vehicle
STZ
Rin 30 30 0
Ang (1-7) (pmol)
1 1
A779 (nmol)

Figure 3

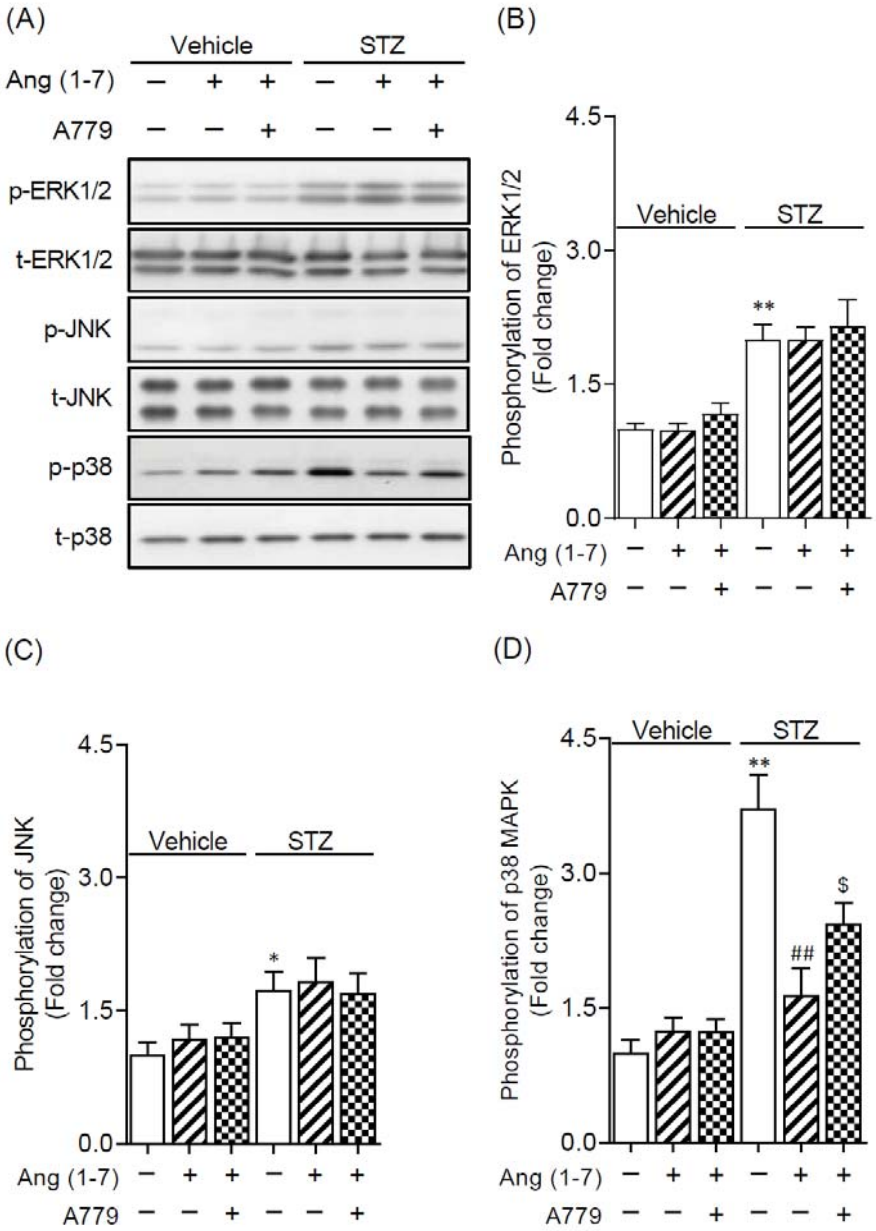
(A)
Vehicle
STZ
Ang (1-7) – + + – + +
A779 – – + – – +
p-ERK1/2
t-ERK1/2
p-JNK
t-JNK
p-p38
t-p38
(B)
Phosphorylation of ERK1/2 (Fold change)
4.5
3.0
1.5
0.0
Vehicle
STZ
**
Ang (1-7) – + + – + +
A779 – – + – – +
(C)
Phosphorylation of JNK (Fold change)
4.5
3.0
1.5
0.0
Vehicle
STZ
*
Ang (1-7) – + + – + +
A779 – – + – – +
(D)
Phosphorylation of p38 MAPK (Fold change)
4.5
3.0
1.5
0.0
Vehicle
STZ
**
##
$
Ang (1-7) – + + – + +
A779 – – + – – +

Figure 4

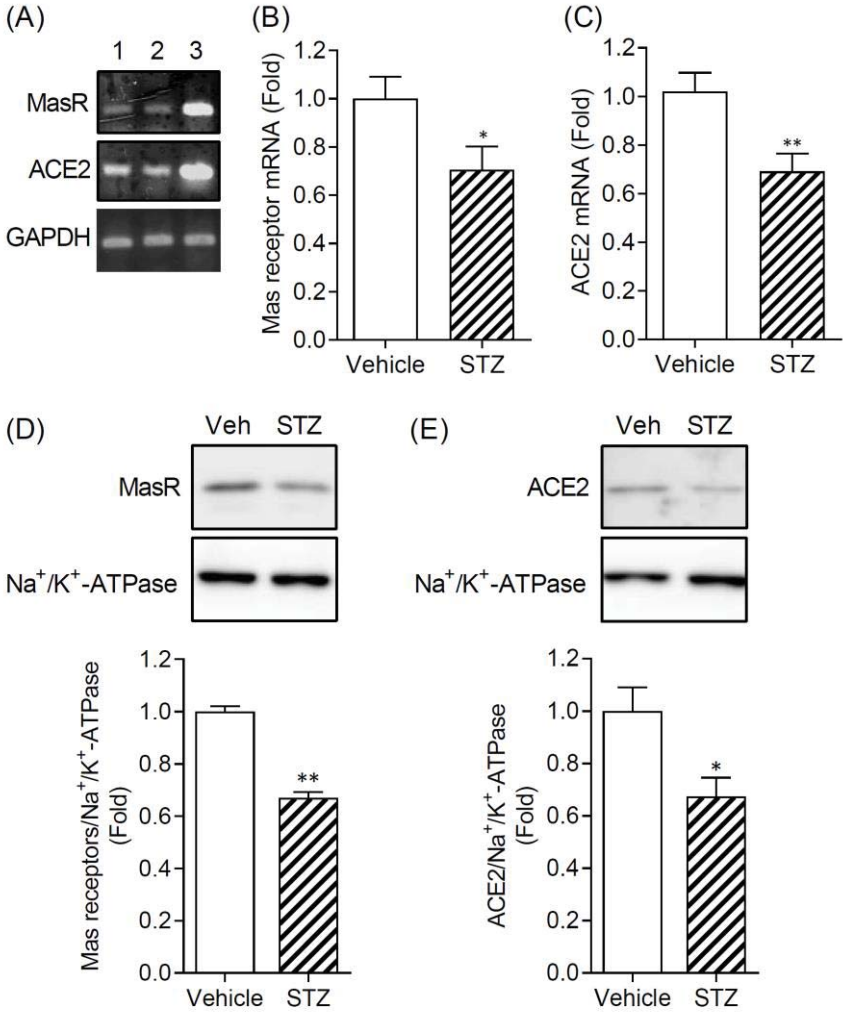
(A)
1 2 3
MasR
ACE2
GAPDH
(B)
Mas receptor mRNA (Fold)
1.2
1.0
0.8
0.6
0.4
0.2
0.0
*
Vehicle
STZ
(C)
ACE2 mRNA (Fold)
1.2
1.0
0.8
0.6
0.4
0.2
0.0
**
Vehicle
STZ
(D)
Veh
STZ
MasR
Na+/K+-ATPase
Mas receptors/Na+/K+-ATPase (Fold)
1.2
1.0
0.8
0.6
0.4
0.2
0.0
**
Vehicle
STZ
(E)
Veh
STZ
ACE2
Na+/K+-ATPase
ACE2/Na+/K+-ATPase (Fold)
1.2
1.0
0.8
0.6
0.4
0.2
0.0
*
Vehicle
STZ

Supplementary figure legends

Figure S1. Effect of the i.t. injection of Ang (1-7) on the paw withdrawal threshold in vehicle- and STZ-injected mice. Ringer's solution or Ang (1-7) was administered 90 min prior to measurements. Two-way ANOVA: treatment ($F_{2,65} = 9.03$, $p < 0.05$), group ($F_{1,65} = 32.66$, $p < 0.01$), treatment × group ($F_{2,65} = 3.89$, $p < 0.05$). One-way ANOVA: $F_{5,65} = 11.89$, $p < 0.01$. Values represent the means ± S.E.M. for 11-12 mice. $^{**}p < 0.01$ compared with Ringer injected vehicle mice and $^{\#\#}p < 0.01$, $^{\#}p < 0.05$ compared with Ringer-injected STZ mice.

Figure S2. Changes in phospho-MAPKs in the DRG of STZ mice. DRG samples (L4-L6) were taken 14 days after STZ injection. Phosphorylation of (A) JNK, (B) ERK1/2 and (C) p38 MAPK was examined by Western Blotting. Top: representative Western blots showing the respective phospho- and total-MAPK. Bottom: relative quantification of phospho-MAPKs to total MAPKs set as 1.0 in the vehicle mice. Values represent the means ± S.E.M. for 5 mice.

Figure S3. Changes in Mas receptors in the DRG of STZ mice. DRG samples (L4-L6) were taken 14 days after STZ injection. Expression of Mas receptors and α-tubulin was examined by Western Blotting. Top: representative Wester blots showing Mas receptors

and α-tubulin. Bottom: relative quantification of Mas receptors to α-tubulin set as 1.0 in the vehicle mice. Values represent the means ± S.E.M. for 5mice.

Figure S1

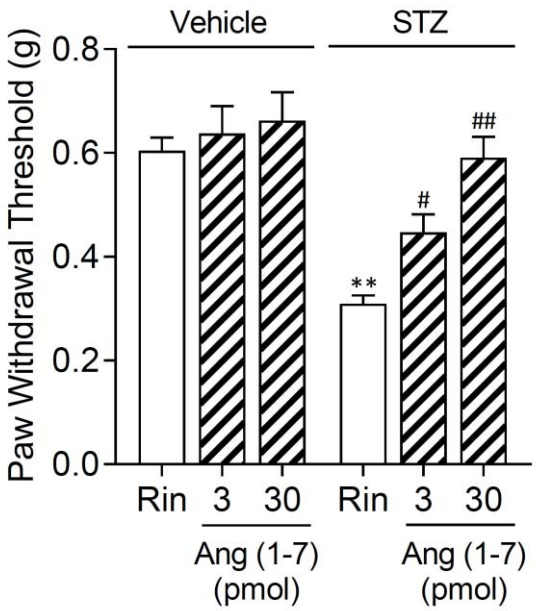
Vehicle
STZ
Paw Withdrawal Threshold (g)
0.0
0.2
0.4
0.6
0.8
**
#
##
Rin
3
30
Rin
3
30
Ang (1-7)
(pmol)
Ang (1-7)
(pmol)

Figure S2

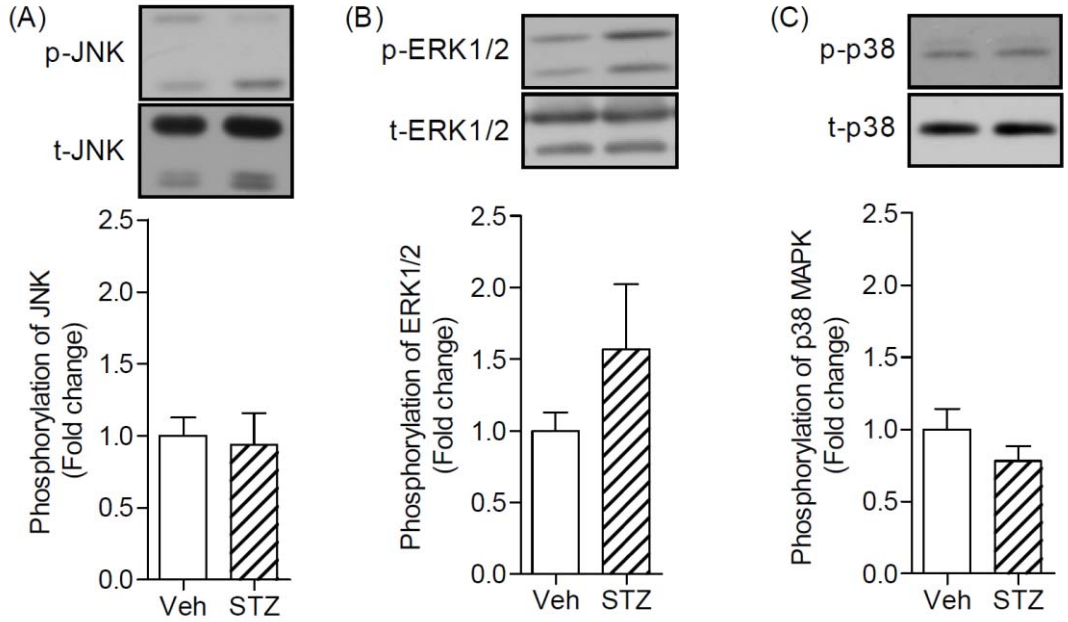
(A)
p-JNK
t-JNK
Phosphorylation of JNK (Fold change)
2.5
2.0
1.5
1.0
0.5
0.0
Veh
STZ
(B)
p-ERK1/2
t-ERK1/2
Phosphorylation of ERK1/2 (Fold change)
2.5
2.0
1.5
1.0
0.5
0.0
Veh
STZ
(C)
p-p38
t-p38
Phosphorylation of p38 MAPK (Fold change)
2.5
2.0
1.5
1.0
0.5
0.0
Veh
STZ

Figure S3

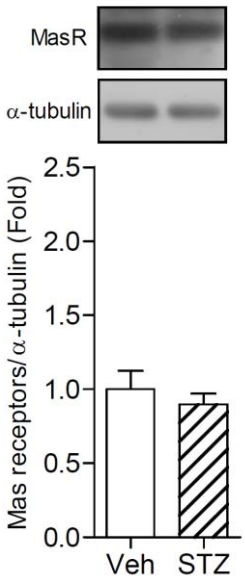
MasR
α-tubulin
Mas receptors/α-tubulin (Fold)
2.5
2.0
1.5
1.0
0.5
0.0
Veh
STZ